ANTIOXIDANTS & REDOX SIGNALING
Volume 14, Number 1, 2011
© Mary Ann Liebert, Inc.
DOI: 10.1089/ars.2010.3539

Does Cellular Hydrogen Peroxide Diffuse or Act Locally?

Natalia M. Mishina,[1,4,*] Pyotr A. Tyurin-Kuzmin,[2,*] Kseniya N. Markvicheva,[1] Alexander V. Vorotnikov,[2] Vsevolod A. Tkachuk,[2] Vibor Laketa,[3] Carsten Schultz,[3] Sergey Lukyanov,[1,4] and Vsevolod V. Belousov[1,4]

Abstract

Understanding of redox signaling requires data on the spatiotemporal distribution of hydrogen peroxide (H_2O_2) within the cell. The fluorescent reporter HyPer is a powerful instrument for H_2O_2 imaging. However, rapid diffusion of HyPer throughout the nucleocytoplasmic compartment does not allow visualization of H_2O_2 gradients on the micrometer scale. Here we dramatically improved the spatial resolution of H_2O_2 imaging by applying subcytoplasmic targeting of HyPer. The membrane-attached reporters identified "microdomains" of elevated H_2O_2 levels within the cytoplasm of the cells exposed to growth factors. We demonstrate that diffusion of H_2O_2 across the cytoplasm was strongly limited, providing evidence that H_2O_2 acts locally inside cells. *Antioxid. Redox Signal.* 14, 1–7.

Introduction

CELLS CONTINUOUSLY PRODUCE reactive oxygen species (ROS). Among ROS, superoxide anion radicals, hydroxyl radicals, hydrogen peroxide (H_2O_2), and nitric oxide are the most investigated species in biology (7). ROS are responsible for oxidative damage of DNA, proteins, and lipids and are associated with disease states such as inflammation, cancer, and neurodegenerative diseases, among others. Physiological processes, such as aging, differentiation, cell motility, and others, are known to be significantly associated with intracellular ROS production.

A decade ago, H_2O_2 was positively identified as a messenger molecule acting through selective modification of thiol groups in proteins regulating signal transduction from growth factor and cytokine receptors (16, 20). H_2O_2 is not a radical; therefore, it is less reactive and, hence, much more stable than other ROS (21). H_2O_2 is small enough to travel over long distances within or even between cells. Although the degree of permeability of biomembranes for H_2O_2 is still under debate (4), properties of H_2O_2 such as its transient appearance make this molecule a good candidate for being a "messenger." However, lack of data on spatiotemporal mapping of H_2O_2 at the level of cellular subcompartments significantly challenges the understanding of its role and regulation in signaling and disease.

Intracellular H_2O_2 production can be efficiently visualized with fluorescent probes, based on either small molecules (14) or genetically encoded constructs (3, 10). The first provides the advantages of simplicity and high signal-to-background ratio, whereas the second class of sensors give often higher specificity and avoid cumbersome chemistry. Reversibility of the genetically encoded probes enables real-time imaging of the H_2O_2 dynamics. Currently, two genetically encoded H_2O_2 sensors are available. One is HyPer (3) and the other is Orp1-redox-sensitive green fluorescent protein 2 (roGFP2) (10). HyPer is based on circularly permuted yellow fluorescent protein (YFP) inserted into the regulatory domain of the *Escherichia coli* OxyR protein. It reacts directly with submicromolar H_2O_2 by forming a disulphide bridge, which leads to conformational changes in the protein and, hence, to a YFP spectral change. In the Orp1-roGFP2 fusion, the peroxidase Orp1 oxidizes a cysteine in roGFP2 using H_2O_2 as a substrate. The resulting disulphide changes the roGFP2 β-barrel structure, leading to spectral changes. However, spatial resolution of the H_2O_2 signal imaged with both genetically encoded probes is low. The rapid diffusion of the sensor within the nucleocytoplasmic compartment delocalizes the signal even in the case of local H_2O_2 production.

Peptide growth factors stimulate cellular response *via* activation of receptor tyrosine kinases (RTKs) localized on the plasma membrane (PM) of cells (19), followed by phosphorylation of various downstream targets. Ligand-bound receptors become rapidly internalized into endosomes and are subsequently either degraded or recycled to the PM (17). Protein tyrosine phosphatase (PTP-1B) attached to the cytosolic face of the endoplasmic reticulum (ER) membrane *via* a C-terminal "tail anchor" sequence (1) is responsible for

[1]Shemyakin-Ovchinnikov Institute of Bioorganic Chemistry, Moscow, Russia.
[2]Faculty of Basic Medicine, Moscow State University, Moscow, Russia.
[3]EMBL Heidelberg, Heidelberg, Germany.
[4]Nizhny Novgorod State Medical Academy, Nizhny Novgorod, Russia.
*These two authors contributed equally to this work.

dephosphorylation of many RTKs, including epidermal growth factor receptor (EGFR) and platelet-derived growth factor receptor (PDGFR) (9, 11), especially after internalization (22), and helps switching off the kinase cascade. To allow the propagation of RTK activity, it is necessary to inhibit PTPs including PTP-1B. Cells extensively utilize H_2O_2 to control PTP activity *via* reversible oxidation of their active site thiolates (6, 13, 18). Although PTP-1B oxidation by H_2O_2 was shown both *in vitro* and *in vivo* (6, 12), the mechanism of oxidation of this and other PTPs remains enigmatic. It is not clear how PTPs, which have a rate constant of reaction with H_2O_2 ranging from 10 to 10^3 M^{-1} s^{-1}, compete effectively with the abundant peroxiredoxins with rate constants up to 2×10^7 M^{-1} s^{-1}. A growing body of evidence suggests, therefore, a model of compartmentalized redox signaling. According to this model, thiolate-containing targets are oxidized by H_2O_2 produced by neighboring NADPH oxidase (Nox) family enzymes residing in the same subcompartment. In this case, the local H_2O_2 concentration could be high enough to temporarily oxidize any nearby peroxiredoxins, allowing further oxidation of PTPs (21). This model, however, requires experimental verification by monitoring real-time dynamics of H_2O_2 production in various cellular compartments upon RTKs activation. An especially controversial issue is which cellular compartment is responsible for Nox activation and H_2O_2 production. The PM, the endosomal compartment, or even the ER membrane are candidates, because all of these compartments have been shown to contain Nox (2, 5).

Therefore, we decided to improve the spatial resolution of H_2O_2 imaging by developing an imaging platform based on immobilized HyPer. We immobilized HyPer probes within certain subcompartments in the cytoplasm and used this strategy to identify localization of the H_2O_2 signal during activation of RTKs. We demonstrated that H_2O_2 produced in RTK signaling does not diffuse freely across the cytoplasm, but instead localizes to microdomains near the sites of its generation.

Results, Discussion, and Future Directions

We proposed that H_2O_2 generation should colocalize with either activated receptor or PTP-1B, or both. To evaluate the first possibility, we targeted HyPer to the PM and endosomes by fusing it with the C-termini of EGFR and PDGFR, and the EGFR (1-1210)-HyPer and PDGFR (1-1106)-HyPer fusions were expressed in HeLa and NIH-3T3 cells, respectively. Upon serum starvation, most of the fluorescence was localized at the PM in both cell types. In many NIH-3T3 cells, PDGFR-HyPer localized both at the PM and in endosome-like endomembranes (Supplementary Fig. 1; *see* www.liebertonline.com/ars).

Stimulation of HeLa cells with EGF resulted in internalization of EGFR-HyPer into endocytic vesicles (Fig. 1A; Supplementary Video 1; *see* www.liebertonline.com/ars). Importantly, a fraction of the fluorescence retained at its initial membrane localization reflects the noninternalized receptors. We observed that a substantial elevation of H_2O_2 levels in the endosomal fraction started within 7–10 min after stimulation. H_2O_2 concentrations reached a plateau within the next 10–15 min, followed by the second wave of H_2O_2 production (Fig. 1C). However, the fraction of the probe residing at the PM demonstrated no increase in F500/F420 ratio. In fact, the probe associated with the PM became more reduced, suggesting either termination of H_2O_2-producing activity on the PM or translocation of the H_2O_2-generating system from PM to the endosomes. This observation suggested that the endosomes containing internalized receptor served as the compartment responsible for H_2O_2 generation. Addition of the Nox inhibitor diphenyleniodonium (DPI) at concentrations as low as 5 μM rapidly and completely inhibited H_2O_2 production, indicating Nox as a most likely source of ROS in endosomes (Supplementary Fig. 2; *see* www.liebertonline.com/ars). The absence of PM-associated HyPer oxidation demonstrated that, first, there was no Nox activation and ROS production on the PM and, second, the diffusion volume of H_2O_2 is limited to a few micrometers. Indeed, in case H_2O_2 would diffuse freely across the cytoplasm, PM-associated HyPer would be oxidized by H_2O_2 produced by endosomes. Importantly, HyPer ratio values often differ between neighboring endosomes (Fig. 1B, D), arguing for the strict limitation of H_2O_2 diffusion. Therefore, we suspect that cellular antioxidant systems degrade H_2O_2 before it is able to reach distant compartments.

H_2O_2 is generated upon activation of many different RTKs. However, it is not known if the spatiotemporal patterns of H_2O_2 production differ between cell types expressing different receptors. To address this question, we stimulated NIH-3T3 fibroblasts expressing PDGFR-HyPer with PDGF. In contrast to EGFR-HyPer–expressing HeLa cells, we did not observe intensive internalization of PDGFR-HyPer into endosomes, but rather intensive filopodia formation and changes of the cell shape in response to the stimulus. The spatiotemporal pattern of H_2O_2 generation also differed from that in HeLa cells. In PDGFR-HyPer–expressing cells, the majority of H_2O_2 production was associated with the PM (Fig. 2A; Supplementary Video 2; *see* www.liebertonline.com/ars), including filopodia (Fig. 2B, C, E; Supplementary Video 3; *see* www.liebertonline.com/ars). H_2O_2 started to rise within 1 min after PDGF addition (Fig. 2D, E) and peaked after 10 min, followed by partial reduction of the probe within the next 10 min and the subsequent start of the second H_2O_2 wave (Fig. 2D). Fluorescence of HyPer associated with PDGFR-containing endomembranes remained almost unchanged during the first 20 min after stimulation and then started to rise (Fig. 2D). This showed that PM contained the pool of active Nox in NIH-3T3 cells upon RDGFR stimulation. The absence of diffusion of H_2O_2 from the PM to endomembranes, at least below some [H_2O_2] threshold at the PM, resembled that in HeLa cells, indicating rapid degradation of H_2O_2 by intracellular oxidant defense systems. The elevation of H_2O_2 in 3T3-NIH fibroblasts appeared to be DPI sensitive, supporting that Nox may function as a source of ROS (data not shown).

Being a target of H_2O_2, phosphatase PTP-1B becomes oxidized during RTK activation (12, 13). Membranes hosting activated EGFR and PDGFR have been previously shown to contact with microdomains of PTP-1B–containing ER membrane where receptor dephosphorylation occurs (11). At the same time, membranes containing activated receptors also possessed strong H_2O_2 production, likely because of Nox activity (Figs. 1 and 2), for PTP-1B inhibition. Another possible source of H_2O_2 for PTP-1B oxidation was the ER-residing Nox pool. We proposed that [H_2O_2] dynamics at the ER membrane could provide some information to support either ER or non-ER Nox to be a source of the oxidant. For this

purpose, we produced HyPer-tail anchor (TA), HyPer targeted to the cytoplasmic surface of the ER membrane, by fusing the indicator with the TA of PTP-1B (24 C-terminal amino acid residues) (Supplementary Fig. 1). When expressed in HeLa and NIH-3T3 cells, HyPer-TA localized to the ER (Fig. 3 and Supplementary Fig. 1), demonstrating the same localization pattern as the EYFP-tagged PTP-1B (1) and recently reported HyPer-ERcyto construct (8). Upon stimulation of EGFR in HeLa cells, HyPer-TA detected increases of H_2O_2 near the ER membrane (Fig. 3A; Supplementary Video 4; *see* www.liebertonline.com/ars). However, the temporal pattern of the fluorescent response differed from that of EGFR-HyPer. The first wave of H_2O_2 started with less than a minute delay after the stimulus and lasted for 10–15 min before a second wave of H_2O_2 of much higher amplitude followed (Fig. 3C). This second wave of HyPer-TA oxidation reflected either direct ER-produced H_2O_2 or, alternatively, the endosomal pool of the oxidant reaching the ER membrane. The first H_2O_2 peak, despite being of low amplitude, started before the endosome-associated H_2O_2 pool became detectable. This indicated that the ER-associated H_2O_2 production becomes activated faster than endosomal H_2O_2 appears.

Addition of PDGF to the NIH-3T3 cells expressing HyPer-TA caused a significant change in the probe ratio, reflecting intensive H_2O_2 production near the ER of the fibroblasts (Fig. 3B; Supplementary Video 5; *see* www.liebertonline.com/ars). The shape and amplitude of H_2O_2 change closely resembled those observed on the PM using PDGFR-HyPer (compare Fig. 3D with Fig. 2D). Together with the observation that the HyPer ratio at the PDGFR-containing endomembranes remained unchanged at the same time (Fig. 2D), HyPer-TA oxidation suggests the existence of a specific ER-residing Nox pool.

Immobilized HyPer variants, unlike the nontargeted probe, allow a significant enhancement of the spatial resolution in H_2O_2 imaging. Using this approach, we demonstrated for the first time the microdomains of H_2O_2 production in RTK signaling. Upon activation of EGFR in HeLa cells, a substantial amount of H_2O_2 was generated on endosomes. Therefore, endosomes carrying internalized EGFR possess both activities required for maintaining downstream target phosphorylation after tyrosine kinase activation: RTK phosphorylates substrates, whereas Nox releases ROS exactly at the same place, inhibiting PTPs and other targets. Such endosomes represent powerful functional units of intracellular EGFR and redox signaling. Rapid rises of H_2O_2 at the ER might be necessary for the immediate inhibition of PTP-1B on these membranes. However, the mechanism required for the initial activation of ER-resident Nox remains to be identified.

The absence of PM-associated HyPer oxidation in HeLa cells suggests that H_2O_2 production and many of the H_2O_2 targets are localized within the cell. In contrast, activation of Nox at the PM in fibroblasts argues for possible extracellular targets of H_2O_2 produced upon PDGFR activation (15). Indeed, as the diffusion of H_2O_2 within the cytoplasm is limited to a few microns, H_2O_2 for paracrine signaling should be produced by PM-residing Nox.

Oxidation of HyPer-TA in both EGFR and PDGFR signaling provides a reliable model to study the PTP-1B inhibition by H_2O_2. Comparison of timing and amplitude of HyPer-TA oxidation with that of EGFR-HyPer and PDGFR-HyPer fusions revealed a high probability of ER-resident Nox activation in both cell types. For PDGFR signaling in NIH-3T3 fibroblasts, Nox in the ER could be the major source of PTP-1B inhibition because of the apparent absence of receptor internalization and the limitation of intracellular H_2O_2 diffusion.

Taken together, imaging by immobilized HyPer variants in complementation with recent research on tissue-scale H_2O_2 patterning (15) shows how biological systems control highly reactive and diffusible molecules and use them for signaling.

Materials and Methods

Materials

H_2O_2, DPI, EGF, and PDGF-BB were purchased from Sigma. Dulbecco-phosphate-buffered saline, Dulbecco's modified Eagle's medium, Opti–minimal essential medium (MEM), MEM, fetal calf serum, and FuGene6 transfection reagent were from Invitrogen. Glass-bottomed dishes were from MatTec. NIH-3T3 cells were from ATCC. HeLa-Kyoto cell line was provided by EMBL. Encyclo PCR kit and HyPer expression vectors were from Evrogen. Restriction endonucleases were from SibEnzyme.

Methods

Preparation of fusion constructs. To make EGFR-HyPer, the YFP-coding region of pEGFR-YFP vector was replaced with the coding region of Hyper. Hyper was amplified from pHyPer-cyto (Evrogen) with the primers 5′-ATCTCGATCG GTGGAGGTGGAGGAGGCGAGATGGCGAGCCAGCAG-3′ and 5′-CGCAGCGGCCGCTTAAACCGCCTGTTTTAAA ACT-3′; the PCR product was digested with *Pvu*I and *Not*I and cloned into EGFR-YFP in place of YFP.

PDGFR-HyPer was produced by replacing the GFP-coding region of PDGFR-GFP by HyPer-coding DNA amplified from HyPer-cyto vector using the primers 5′-ATCTGGTACCGA GCTCGGATCCATGGAGATGGCGAGCCAGCAGG-3′ and 5′-CGCATCTAGATTAAACCGCCTGTTTTAAAACTTTAT CG-3′ coding the restriction sites of *Kpn*I and *Xba*I.

For HyPer-TA construction, DNA encoding residues 412–435 of PTP1B was amplified from pPTP1B-YFP vector using the primers 5′-ATCTCTCGAGCTAACATGTGCGTGGCTA CGGT-3′ and 5′-CGCAGGATCCCTATGTGTTGCTGTTGA ACAG-3′. The PCR product was digested with *Xho*I and *Bam*HI and cloned into pHyPer-NLS vector.

All constructs were confirmed by sequence analysis.

Cell culture and transfection. HeLa-Kyoto and NIH-3T3 cells were cultured in Dulbecco's modified Eagle's medium supplemented with 10% fetal calf serum at 37°C in an atmosphere containing 95% air and 5% CO_2. Cells were split every second day and seeded on glass-bottomed dishes. Twenty-four hours later, cells were transfected with a mixture of vector DNA and FuGene6 transfection reagent according to the manufacturer's recommendations.

Stimulation of the cells and imaging. Twenty-four hours after transfection, the culture medium was changed to MEM without phenol red and serum. After 2 h (HeLa-Kyoto) or 6 h (NIH-3T3) of incubation, the glass-bottomed dishes were transferred onto the microscopic stage of either a confocal (laser scanning confocal inverted microscope Carl Zeiss LSM 510-META or PerkinElmer Ultraview VoX confocal inverted microscope) or a widefield (Leica 6000) microscope equipped with an HCX PL APO lbd.BL 63×1.4NA oil objective and an environmental chamber (EMBL). HyPer fluorescence was

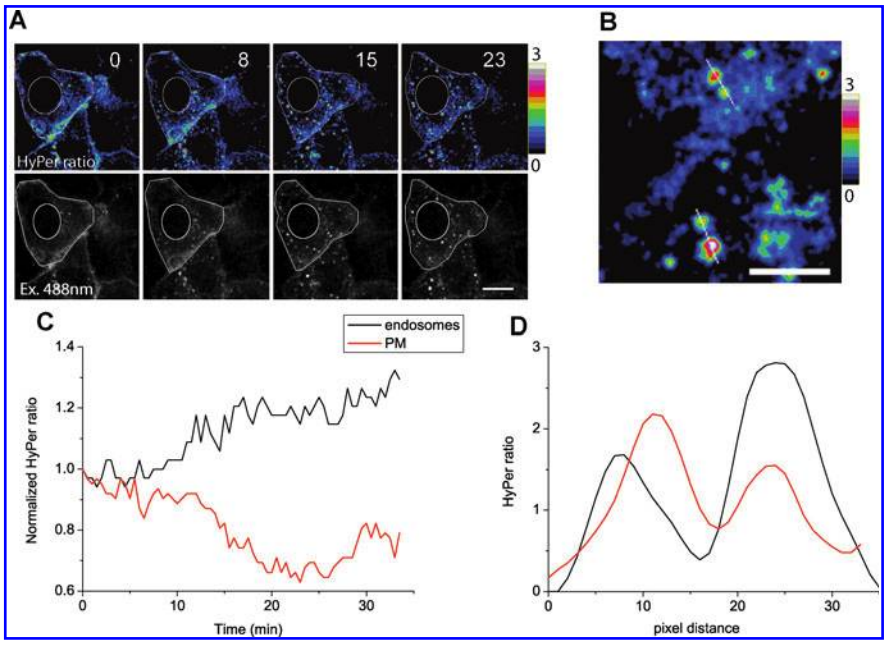

FIG. 1. Microdomains of elevated H_2O_2 generation upon activation of EGFR. (A) Confocal images of EGFR-HyPer–expressing HeLa-Kyoto cells at indicated time points (in minutes) after stimulation of the cells with 50 ng/ml EGF. Upper row of images represent subcellular distribution of HyPer ratio. Lower row of images show subcellular distribution of EGFR-HyPer. Cell boundaries and nucleus of one of the cells are highlighted. Scale bar: 15 μm. **(B)** Confocal image of a selected region inside the cell containing internalized receptor. Image represents HyPer ratio values. Note that neighboring endosomes demonstrate different HyPer ratio. Signal intensity profiles along the lines are shown on **(D)**. Scale bar: 5 μm. **(C)** Time course of H_2O_2 production associated with endosomes and PM in the cells shown on **(A)**. **(D)** HyPer ratio values along the upper (red) and lower (black) lines shown on **(B)**. The figure is representative of 37 cells from three experiments. H_2O_2, hydrogen peroxide; PM, plasma membrane; EGFR, epidermal growth factor receptor. (For interpretation of the references to color in this figure legend, the reader is referred to the web version of this article at www.liebertonline.com/ars).

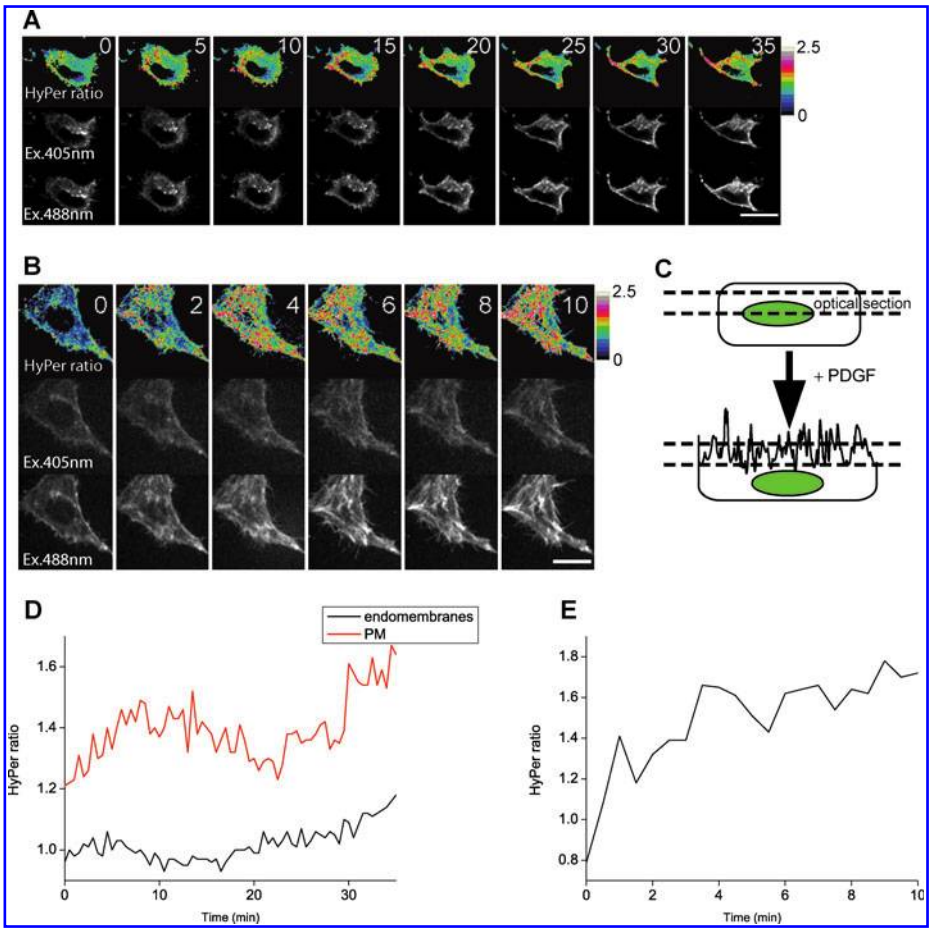

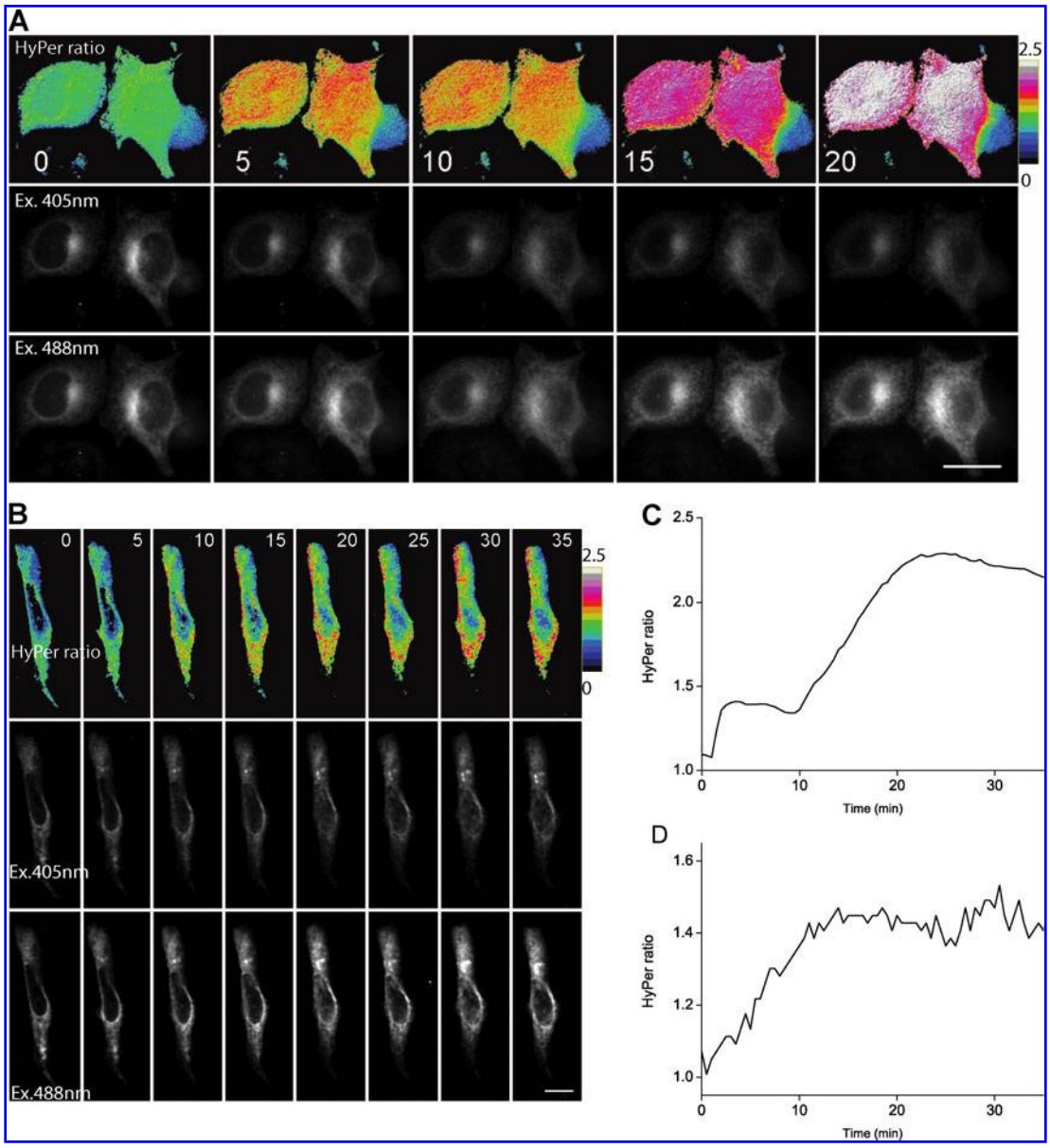

FIG. 3. Dynamics of H_2O_2 near the cytoplasmic surface of the endoplasmic reticulum membrane upon activation of the cells with growth factors. (A) Widefield fluorescence images of HyPer-TA–expressing HeLa-Kyoto cells at indicated time points (in minutes) after stimulation of the cells with 50 ng/ml EGF. Upper row of images represent subcellular distribution of HyPer ratio. Middle and lower rows of images show subcellular distribution of HyPer-TA and changes in fluorescence intensity in each imaging channel. Scale bar: 15 μm. **(B)** Confocal images of HyPer-TA–expressing cells at indicated time points (in minutes) after stimulation of the cells with 10 ng/ml PDGF. Upper row of images represent subcellular distribution of HyPer ratio. Middle and lower rows of images show subcellular distribution of HyPer-TA and changes in fluorescence intensity in each imaging channel. Scale bar: 10 μm. **(C)** Time course of H_2O_2 production by the cells shown on **(A)**. **(D)** Time course of H_2O_2 production by the cell shown on **(B)**. The figure is representative of 11 HeLa-Kyoto cells from three experiments and 43 NIH-3T3 cells from three experiments. TA, tail anchor. (For interpretation of the references to color in this figure legend, the reader is referred to the web version of this article at www.liebertonline.com/ars).

FIG. 2. Microdomains of elevated H_2O_2 generation upon activation of PDGFR. (A) Confocal images of PDGFR-HyPer–expressing NIH-3T3 cell at indicated time points (in minutes) after stimulation of the cells with 10 ng/ml PDGF. Upper row of images represent subcellular distribution of HyPer ratio. Lower rows of images show subcellular distribution of EGFR-HyPer and fluorescence intensities in two imaging channels excited with 405 and 488 nm lasers (see Materials and Methods section for details). Scale bar: 15 μm. **(B)** H_2O_2 generation in filopodia of PDGFR-HyPer–expressing NIH-3T3 cell after stimulation with PDGF. Scale bar: 15 μm. **(C)** Illustration of the events visible on **(B)**. Upon addition of PDGF, cell starts changing its shape. This results in simultaneous movement of the nucleus away from the confocal optical section and appearance of the "dorsal" PM in the optical slice. At this moment, intensive filopodia formation on the PM is clearly visible as well as production of H_2O_2 by the receptor localized on PM. **(D)** Time course of H_2O_2 production by receptor-containing endomembranes and PM in the cell shown on **(A)**. **(E)** Time course of H_2O_2 production by filopodia of stimulated NIH-3T3 cell shown on **(B)**. The figure, except **(B)**, **(C)**, and **(E)**, is representative of 27 cells from three experiments. PDGFR, platelet-derived growth factor receptor. (For interpretation of the references to color in this figure legend, the reader is referred to the web version of this article at www.liebertonline.com/ars).

excited sequentially with 405 and 488 nm lasers of confocal fluorescent microscope or 427/10 and 504/12 band-pass excitation filters of the widefield fluorescent microscope. Emission of the probe was collected every 30 s using a 527W55 band-pass emission filter of the confocal system or a 525/50 band-pass emission filter of the widefield fluorescent microscope. After 3–5 images were acquired, 50 ng/ml EGF or 10 ng/ml PDGF was added.

Time series processing. Time series were analyzed using ImageJ free software downloaded from EMBL ALMF website (www.embl.de/almf/). For confocal images, 420- and 500-nm stacks (correspond to two HyPer excitation peaks) were Gaussian filtered and the background was subtracted. Images were converted to 32 bits and a 420-nm stack was thresholded to remove pixel values from background (Not-a-Number function). A 500-nm stack was divided into a 420-nm stack frame-by-frame. The resulting stack was depicted in pseudocolors using a "Ratio" lookup table. Time course of HyPer fluorescence was calculated for regions of interest inside the imaged cell.

To calculate average HyPer ratio values in the endosomes, we used the fact that the ratio in endosomes is higher than the ratio associated with the PM. Therefore, we thresholded images eliminating ratio values below 0.7. Upon thresholding, mostly endosomes remained visible in the images. After that, the average ratio values for each frame in the stack were calculated.

Acknowledgments

The authors thank Leica Microsystems, Carl Zeiss, and PerkinElmer for continuous support of the EMBL Advanced Light Microscopy Facility, Yury Belyaev (ALMF, EMBL) for help with image analysis, and Philippe I.H. Bastiaens for providing EYFP-PTP1B–encoding DNA. This work was supported by the Federal Education Agency (project no. P256), a grant from the President of Russian Federation (MK-3567.2009.4), the Russian Academy of Sciences Program in Molecular and Cell Biology, the Russian Foundation for Basic Research (09-04-12235, 10-04-01561), Measures to Attract Leading Scientists to Russian Educational Institutions, the Howard Hughes Medical Institute (55005618), the EU FP6 (LSHG-CT-2003-503259), and the Helmholtz Initiative SBCancer. K.N.M. received FEBS short-term fellowship.

References

1. Anderie I, Schulz I, and Schmid A. Characterization of the C-terminal ER membrane anchor of PTP1B. *Exp Cell Res* 313: 3189–3197, 2007.
2. Bedard K and Krause KH. The NOX family of ROS-generating NADPH oxidases: physiology and pathophysiology. *Physiol Rev* 87: 245–313, 2007.
3. Belousov VV, Fradkov AF, Lukyanov KA, Staroverov DB, Shakhbazov KS, Terskikh AV, and Lukyanov S. Genetically encoded fluorescent indicator for intracellular hydrogen peroxide. *Nat Methods* 3: 281–286, 2006.
4. Bienert GP, Schjoerring JK, and Jahn TP. Membrane transport of hydrogen peroxide. *Biochim Biophys Acta* 1758: 994–1003, 2006.
5. Chen K, Kirber MT, Xiao H, Yang Y, and Keaney JF, Jr. Regulation of ROS signal transduction by NADPH oxidase 4 localization. *J Cell Biol* 181: 1129–1139, 2008.
6. Denu JM and Tanner KG. Specific and reversible inactivation of protein tyrosine phosphatases by hydrogen peroxide: evidence for a sulfenic acid intermediate and implications for redox regulation. *Biochemistry* 37: 5633–5642, 1998.
7. Droge W. Free radicals in the physiological control of cell function. *Physiol Rev* 82: 47–95, 2002.
8. Enyedi B, Varnai P, and Geiszt M. Redox state of the endoplasmic reticulum is controlled by Ero1L-alpha and intraluminal calcium. *Antioxid Redox Signal* 13: 721–729, 2010.
9. Flint AJ, Tiganis T, Barford D, and Tonks NK. Development of "substrate-trapping" mutants to identify physiological substrates of protein tyrosine phosphatases. *Proc Natl Acad Sci USA* 94: 1680–1685, 1997.
10. Gutscher M, Sobotta MC, Wabnitz GH, Ballikaya S, Meyer AJ, Samstag Y, and Dick TP. Proximity-based protein thiol oxidation by H2O2-scavenging peroxidases. *J Biol Chem* 284: 31532–31540, 2009.
11. Haj FG, Verveer PJ, Squire A, Neel BG, and Bastiaens PI. Imaging sites of receptor dephosphorylation by PTP1B on the surface of the endoplasmic reticulum. *Science* 295: 1708–1711, 2002.
12. Lee SR, Kwon KS, Kim SR, and Rhee SG. Reversible inactivation of protein-tyrosine phosphatase 1B in A431 cells stimulated with epidermal growth factor. *J Biol Chem* 273: 15366–15372, 1998.
13. Meng TC, Fukada T, and Tonks NK. Reversible oxidation and inactivation of protein tyrosine phosphatases *in vivo*. *Mol Cell* 9: 387–399, 2002.
14. Miller EW, Tulyathan O, Isacoff EY, and Chang CJ. Molecular imaging of hydrogen peroxide produced for cell signaling. *Nat Chem Biol* 3: 263–267, 2007.
15. Niethammer P, Grabher C, Look AT, and Mitchison TJ. A tissue-scale gradient of hydrogen peroxide mediates rapid wound detection in zebrafish. *Nature* 459: 996–999, 2009.
16. Rhee SG. Cell signaling. H2O2, a necessary evil for cell signaling. *Science* 312: 1882–1883, 2006.
17. Roepstorff K, Grandal MV, Henriksen L, Knudsen SL, Lerdrup M, Grovdal L, Willumsen BM, and van Deurs B. Differential effects of EGFR ligands on endocytic sorting of the receptor. *Traffic* 10: 1115–1127, 2009.
18. Ross SH, Lindsay Y, Safrany ST, Lorenzo O, Villa F, Toth R, Clague MJ, Downes CP, and Leslie NR. Differential redox regulation within the PTP superfamily. *Cell Signal* 19: 1521–1530, 2007.
19. Schlessinger J. Cell signaling by receptor tyrosine kinases. *Cell* 103: 211–225, 2000.
20. Ushio-Fukai M. Localizing NADPH oxidase-derived ROS. *Sci STKE* 2006: re8, 2006.
21. Winterbourn CC. Reconciling the chemistry and biology of reactive oxygen species. *Nat Chem Biol* 4: 278–286, 2008.
22. Yudushkin IA, Schleifenbaum A, Kinkhabwala A, Neel BG, Schultz C, and Bastiaens PI. Live-cell imaging of enzyme-substrate interaction reveals spatial regulation of PTP1B. *Science* 315: 115–119, 2007.

Address correspondence to:
Dr. Vsevolod V. Belousov
Shemyakin-Ovchinnikov Institute of Bioorganic Chemistry RAS, Miklukho-Maklaya 16/10
Moscow 117997
Russia

E-mail: vsevolod.belousov@gmail.com

Date of first submission to ARS Central, August 5, 2010; date of acceptance, August 8, 2010.

Abbreviations Used

DPI = diphenyleniodonium
EGFR = epidermal growth factor receptor
ER = endoplasmic reticulum
H_2O_2 = hydrogen peroxide
MEM = minimal essential medium
Nox = NADPH oxidase
PDGFR = platelet-derived growth factor receptor
PM = plasma membrane
PTP = protein tyrosine phosphatase
roGFP2 = redox-sensitive green fluorescent protein 2
ROS = reactive oxygen species
RTK = receptor tyrosine kinase
TA = tail anchor
YFP = yellow fluorescent protein

This article has been cited by:

1. Subash C. Gupta , David Hevia , Sridevi Patchva , Byoungduck Park , Wonil Koh , Bharat B. Aggarwal . 2012. Upsides and Downsides of Reactive Oxygen Species for Cancer: The Roles of Reactive Oxygen Species in Tumorigenesis, Prevention, and Therapy. *Antioxidants & Redox Signaling* **16**:11, 1295-1322. [Abstract] [Full Text HTML] [Full Text PDF] [Full Text PDF with Links]
2. Marta Armogida, Robert Nisticò, Nicola Biagio Mercuri. 2012. Therapeutic potential of targeting hydrogen peroxide metabolism in the treatment of brain ischaemia. *British Journal of Pharmacology* **166**:4, 1211-1224. [CrossRef]
3. Valeria Gabriela Antico Arciuch , María Eugenia Elguero , Juan José Poderoso , María Cecilia Carreras . 2012. Mitochondrial Regulation of Cell Cycle and Proliferation. *Antioxidants & Redox Signaling* **16**:10, 1150-1180. [Abstract] [Full Text HTML] [Full Text PDF] [Full Text PDF with Links]
4. Christine C. WinterbournBiological Chemistry of Reactive Oxygen Species . [CrossRef]
5. Ting Su, Xiangyong Li, Nisha Liu, Shaotao Pan, Jinling Lu, Jie Yang, Zhihong Zhang. 2012. Real-time imaging elucidates the role of H[sub 2]O[sub 2] in regulating kinetics of epidermal growth factor-induced and Src-mediated tyrosine phosphorylation signaling. *Journal of Biomedical Optics* **17**:7, 076015. [CrossRef]
6. Patricia Back, Bart P. Braeckman, Filip Matthijssens. 2012. ROS in Aging Caenorhabditis elegans: Damage or Signaling?. *Oxidative Medicine and Cellular Longevity* **2012**, 1-14. [CrossRef]
7. A. V. Vorotnikov. 2011. Chemotaxis: Movement, direction, control. *Biochemistry (Moscow)* **76**:13, 1528-1555. [CrossRef]
8. Margaret E. Tome, Melba C. Jaramillo, Margaret M. Briehl. 2011. Hydrogen peroxide signaling is required for glucocorticoid-induced apoptosis in lymphoma cells. *Free Radical Biology and Medicine* . [CrossRef]
9. Bryan C. Dickinson, Yan Tang, Zengyi Chang, Christopher J. Chang. 2011. A Nuclear-Localized Fluorescent Hydrogen Peroxide Probe for Monitoring Sirtuin-Mediated Oxidative Stress Responses In Vivo. *Chemistry & Biology* **18**:8, 943-948. [CrossRef]
10. Bryan C Dickinson, Christopher J Chang. 2011. Chemistry and biology of reactive oxygen species in signaling or stress responses. *Nature Chemical Biology* **7**:8, 504-511. [CrossRef]
11. Elizabeth Veal , Alison Day . 2011. Hydrogen Peroxide as a Signaling Molecule. *Antioxidants & Redox Signaling* **15**:1, 147-151. [Abstract] [Full Text HTML] [Full Text PDF] [Full Text PDF with Links]
12. Sarah L. Cuddihy , Christine C. Winterbourn , Mark B. Hampton . 2011. Assessment of Redox Changes to Hydrogen Peroxide-Sensitive Proteins During EGF Signaling. *Antioxidants & Redox Signaling* **15**:1, 167-174. [Abstract] [Full Text HTML] [Full Text PDF] [Full Text PDF with Links] [Supplemental material]